Modeling Crowd Evacuation via Behavioral Heterogeneity-Based Social Force Model

Wenhan Wu, Jinghai Li, Wenfeng Yi, and Xiaoping Zheng

Abstract— **With the increasing scale of crowds in public places, the study of modeling crowd evacuation has become a significant research field. However, most previous research ignores to incorporate behavioral heterogeneity of individuals into the modeling framework, making it hard to replicate more realistic evacuation processes. Therefore, a behavioral heterogeneity-based social force model (BHSFM) is proposed to reveal the heterogeneity characteristics from the aspect of individual behavior. Numerical experiments show that the BHSFM provides a general mathematical framework for describing behavioral heterogeneity and forms a more reasonable and elaborate evacuation process. Notably, some interesting evacuation phenomena can emerge by integrating the behavioral heterogeneity coefficient with temporal-spatial dynamic risk indexes. Compared with the social force model (SFM), higher frequencies of small-scale displacements are performed by BHSFM due to more pushing behaviors. Furthermore, the periods and areas of a potential crowd disaster are revealed by our model under different numbers of pedestrians, which has important guiding significance for formulating reasonable evacuation schemes in specific scenarios.**

Index Terms— **Crowd dynamics, social force model, behavioral heterogeneity, crowd evacuation, nonlinear system.**

I. Introduction

IT IS well-known that the process of crowd evacuation is complicated and risky, there is an urgent need to address corresponding traffic and safety problems [1]. However, evacuation drills and controlled experiments are difficult to reproduce real human collective behaviors under emergency conditions, which brings great challenges to the study of crowd evacuation [2]. Fortunately, the research field of computational social science, which involves different disciplines such as physics, sociology, biology, behavioral science and computer science, etc., has already brought key insights about the modeling of crowd evacuation [3]. Therefore, establishing a more realistic model for crowd evacuation in emergency situations is a significant issue.

Different theories exist in literatures regarding simulation models of crowd evacuation, which have been developed following two directions. One direction emphasizes that large-scale crowds can be modeled analogously to gas kinetics or fluid dynamics [4], whose movements are described by partial differential equations like the Boltzmann-like equations [5] and the Navier-Stokes equations [6]. This kind of model effectively reveals the collective patterns of crowds from a macroscopic perspective, but more detailed characteristics of individuals are neglected [7]. Another opposite direction is modeling crowd evacuation from a microscopic aspect, and typical microscopic models cover the queueing model [8], social force model (SFM) [9], cellular automata model [10], and lattice gas model [11]. These models are beneficial to elucidate the behaviors and interactions between individuals [12], which successfully depict a lot of interesting self-organization phenomena [13] found in empirical observation such as the herding effect [14], freezing by heating [15], and stop-and-go waves [16], [17]. Despite all this, little is known about how the behavioral heterogeneity of pedestrians performs in the above-mentioned models, which is essential to precisely characterize the process of crowd evacuation.

Understanding the heterogeneity characteristics in collective motion has been an active field of research [18], [19]. In terms of experimental studies, Cao *et al.* [20] performed well-controlled experiments to reveal the influence of age heterogeneity on pedestrian dynamics. Fujita *et al.* [21] designed experiments on pedestrian movement at different speeds and discovered the heterogeneous speed could interfere with spontaneous lane formation. Subaih *et al.* [22] indicated that the differences in gender and culture have an impact on movement features by conducting multiple experiments. With regard to discrete models, Guo *et al.* [23] developed a heterogeneous lattice gas model, in which the update rule depends on the local crowd density and the exit congestion degree. Hrabák *et al.* [24] introduced velocity, aggressiveness, and sensitivity to occupation as heterogeneity features into the cellular automata model. However, the above discrete models lack the accuracy of dynamics, making it difficult to reveal the mechanical mechanism of individual behaviors [25]. Regarding continuous models, Cao *et al.* [26] established an improved SFM that incorporates the difference in the stress level of evacuees based on their specific surrounding environments. Ma *et al.* [27] analyzed nine strategies of assigning the parameter of desired speed in SFM to indicate individual diversity. Nonetheless, these models are often limited to a specific perspective, therefore forming a universal framework for measuring heterogeneity characteristics is

Manuscript received 10 May 2021; revised 5 November 2021; accepted 31 December 2021. Date of publication 25 January 2022; date of current version 12 September 2022. This work was supported in part by the National Key Research and Development Program of China under Grant 2020YFF0304900, in part by the National Major Scientific Research Instrument Development Project under Grant 61927804, and in part by the National Natural Science Foundation of China under Grant 61773233. The Associate Editor for this article was S. Hamdar. *(Corresponding author: Xiaoping Zheng.)*

The authors are with the Department of Automation, Tsinghua University, Beijing 100084, China (e-mail: wwh19@mails.tsinghua.edu.cn; ljhai725@163.com; ywf19@mails.tsinghua.edu.cn; asean@mail.tsinghua.edu.cn).

Digital Object Identifier 10.1109/TITS.2022.3140823

challenging [28]. Recently, Wu *et al.* [29] proposed a pedestrian heterogeneity-based social force model (PHSFM) by introducing the physique and mentality coefficients, whereas it remains unclear how physiology and psychology attributes jointly affect the behavioral heterogeneity. Even less is known about whether there is any general mathematical form of the behavioral heterogeneity [30].

To achieve a microscopic description of the behavioral heterogeneity in modeling crowd evacuation, we develop a behavioral heterogeneity-based social force model (BHSFM). The emergency environments and individual differences in aspects of physiology and psychology are integrated to determine the expression of behavioral heterogeneity coefficient. That is, this coefficient provides a more comprehensive mathematical framework to reveal the characteristics of behavioral heterogeneity by affecting the desired speed of pedestrians. Given that large-scale crowds frequently gather in subway stations, the Heping Xiqiao subway station is selected as a simulation scenario for crowd evacuation in emergency situations. Numerical experiments corroborate that the BHSFM displays a more realistic and elaborate evacuation process, and the behavioral heterogeneity coefficient has a significant impact on crowd evacuation. Influenced by temporal-spatial dynamic risk indexes, the BHSFM successfully achieves interesting phenomena in good agreement with empirical observations. Compared with the SFM, higher frequencies of small-scale displacements simulated by our model are attributed to more pushing behaviors. Moreover, the BHSFM determines the periods and areas of a potential crowd disaster under different numbers of pedestrians, which provides crucial guidance for crowd management in specific scenarios.

The rest of this paper is organized as follows. Section II reviews the conceptions of risk index, physique coefficient, and mentality coefficient. In Section III, the BHSFM is proposed to simulate the behavior heterogeneity of pedestrians during evacuation process. Section IV presents corresponding numerical experiments. Finally, the main conclusions and perspectives for future research are illustrated in Section V.

II. Preliminaries

In this section, we recall the conceptions of risk index, physique coefficient, and mentality coefficient proposed in the previous model [29], which has successfully performed special behavior patterns caused by pedestrian heterogeneity.

A. Risk Index

There is evidence that pedestrian behaviors in response to emergency situations are related to the perceived environmental risks [31]. Therefore, the risk index $\lambda \in [0, 1]$ is introduced as a quantitative indicator to measure the degree of emergency. In this case, the specific value of the risk index λ can be evaluated according to different types and scales of incidents. Note that the risk index λ is closer to 1 if the emergency situation is life-threatening, and otherwise tends to 0 in a non-emergency situation. For simplicity of description, the interval of risk index λ is divided into three parts, including the mild level $\lambda \in [0, 0.3)$, moderate level $\lambda \in [0.3, 0.7]$, and severe level $\lambda \in (0.7, 1]$. The risk index is embedded into the following physique and mentality coefficients to reflect the impact of the environment on pedestrians.

B. Physique Coefficient

The physique coefficient reflects the physiology attributes with high stability, accompanied by a slight fluctuation effect in emergency situations [32]. In this case, the physique coefficient $P_i(t)$ of pedestrian i at time t is approximated by one-dimensional Brownian motion:

$$P_i(t + \Delta t) - P_i(t) \sim \mathcal{N}\left(0, \lambda^2 \Delta t\right) \tag{1}$$

where Δt indicates the time step and $\mathcal{N}(\cdot)$ represents the normal distribution.

Given that the initial circumstances, the Beta distribution is adopted to assign physique coefficients for heterogeneous pedestrians. Assuming a random variable $X_i \sim Beta(\alpha, \beta)$, the probability density function is given by:

$$f_{X_i}(x_i | \alpha, \beta) = \frac{\Gamma(\alpha + \beta)}{\Gamma(\alpha)\Gamma(\beta)} x_i^{\alpha - 1}(1 - x_i)^{\beta - 1} \tag{2}$$

where α and β are positive numbers, $\Gamma(\cdot)$ represents the Gamma function. Then, the physique coefficient of pedestrian i at the initial time t_0 is deduced by transforming the random variable X_i as the location-scale family:

$$g(\mathcal{D}) = \{P_i(t_0) | P_i(t_0) = \mu + \sigma x_i, x_i \in \mathcal{D}\} \tag{3}$$

Here, $g : \mathcal{D} \to \mathcal{R}$ is a mapping function on the interval $\mathcal{D} = [0, 1]$. The location parameter $\mu \in \mathcal{R}_+$ limits the lower bound, and the scale parameter $\sigma \in \mathcal{R}_+$ determines the interval range.

With regard to the fluctuation interval of $P_i(t)$, empirical data in gait dynamics theory [33] provides a reasonable evaluation as $P_i(t) \in [(1 - \Delta_P) P_i(t_0), (1 + \Delta_P) P_i(t_0)]$, where Δ_P represents the maximum fluctuation range.

C. Mentality Coefficient

The mentality coefficient illustrates the state transition of stress, cooperation, and competition, permitting a more elaborate psychology expression in pedestrian heterogeneity. Thus, the mentality coefficient of pedestrian i at time t is expressed as follows:

$$M_i(t) = s_i(t)[(1 - \Delta_M) + 2\Delta_M \psi_i(t)] \tag{4}$$

Here, the stress $s_i(t)$ is defined as a basic state, which can be transformed into cooperation or competition through the state transition function $\psi_i(t)$, and Δ_M represents the maximum mutation. For further aspects regarding Equation (4) are illustrated below.

The stress $s_i(t)$ of pedestrian i consists of environmental risks and panics caused by pedestrian counterflows, which is given by the following:

$$s_i(t) = \exp(\lambda)\left\{[1 - p_i(t)]\delta_i^{nor} + p_i(t)\delta_i^{\max}\right\} \tag{5}$$

Here, $\delta_i^{nor} = v_i^{nor} / v_i^0$ and $\delta_i^{\max} = v_i^{\max} / v_i^0$, where v_i^0 is the initial desired speed in that paper, v_i^{nor} is the desired speed in normal and $v_i^{\max}$ the maximum desired speed in panic. The panic parameter $p_i(t) = 1 - \bar{v}_i(t) / v_i^{nor}$ is used to measure

the impatience, where v_i^{nor} is regarded equivalent to v_i^0 and the same for each pedestrian.

Inspired by the neuron activation response [34], the state transition function $\psi_i(t)$ is expressed by the Sigmoid function:

$$\psi_i(t) = \frac{1}{1+\exp\left[-\eta_i \rho_i(t)/k_M\right]} \tag{6}$$

where k_M indicates its slope, $\rho_i(t)$ is the pedestrian density in the personal zone, defined as the following:

$$\rho_i(t) = n_i(t)/\pi \tilde{r}_i^2 \tag{7}$$

where the shape of the personal zone is a circular area with a radius $\tilde{r}_i \approx 4r_i$, and $n_i(t)$ is the number of pedestrians in this zone. The transition of psychology state occurs when the pedestrian density in the personal zone changes [35]. Besides, the random variable η_i of psychological state selection reads:

$$\eta_i = \begin{cases} +1, & 1-\gamma_i(\lambda) \\ -1, & \gamma_i(\lambda) \end{cases} \tag{8}$$

Here, the cooperation probability $\gamma_i(\lambda)$ of pedestrian i is assumed to follow a Boltzmann-like relation, $\gamma_i(\lambda) = \gamma_0 \exp(-w_i\lambda)$, where γ_0 denotes the cooperation probability in non-emergency situations and w_i is the attenuation rate, whose value is pedestrian dependent.

III. Model

A. Behavioral Heterogeneity Coefficient

The behavioral heterogeneity of pedestrians is comprehensively reflected by the above-mentioned risk index, physique coefficient, and mentality coefficient. However, how to incorporate these factors remains unsettled. In this section, we are committed to exploring an appropriate expression of the behavioral heterogeneity coefficient.

Recall the expression of stress $s_i(t)$ in mentality coefficient, Equation (5) can be decomposed into two parts, which originate from the environment and individuals:

$$s_i(t) = s_i^{env}(t) \times s_i^{ind}(t) \tag{9}$$

where $s_i^{env}(t) = \exp(\lambda)$ denotes the stress from environmental risks, and $s_i^{ind}(t)$ indicates the stress from panics caused by pedestrian counterflows:

$$s_i^{ind}(t) = [1-p_i(t)]\,\delta_i^{nor} + p_i(t)\,\delta_i^{\max} \tag{10}$$

where pedestrian i tends to approach $\delta_i^{\max}$ if the panic parameter $p_i(t)$ increases, and otherwise adapts to δ_i^{nor}.

Defining a scale factor as $\theta_i = \delta_i^{nor}/\delta_i^{\max} = v_i^{nor}/v_i^{\max}$, which is the ratio of the desired speed in normal and the maximum desired speed in panic. Thus, Equation (10) is rewritten in the form as follows:

$$s_i^{ind}(t) = [1-p_i(t)]\,\theta_i\delta_i^{\max} + p_i(t)\,\delta_i^{\max} \tag{11}$$

In general, the scale factor θ_i is a constant. However, $\delta_i^{\max}$ should not be regarded as the same for each pedestrian, because the maximum desired speed $v_i^{\max}$ in panic is constrained by physiology attributes. Naturally, an idea occurs that $\delta_i^{\max}$ is assumed to be positively correlated with the physique coefficient $P_i(t)$, which is defined as a linear form:

$$\delta_i^{\max} = \xi P_i(t) \tag{12}$$

where ξ is a positive correlation factor, and we hold $\xi = 1$ in this article. In this case, $v_i^{\max}$ and v_i^{nor} depend on the physique coefficient of pedestrian i, also the panic parameter $p_i(t)$ is pedestrian dependent. Then, the stress that includes physiology heterogeneity is expressed by:

$$s_i^P(t) = \exp(\lambda)\{[1-p_i(t)]\,\theta_i P_i(t) + p_i(t)\,P_i(t)\} \tag{13}$$

In view of the derivation and discussion of aforementioned equations, the physique coefficient is successfully embedded as a part of the mentality coefficient. Therefore, the behavioral heterogeneity coefficient $H_i(t)$ is defined as follows:

$$H_i(t) = s_i^P(t)\,[(1-\Delta_M) + 2\Delta_M\psi_i(t)] \tag{14}$$

Here, Equation (14) is a more comprehensive expression, revealing the behavioral heterogeneity caused by the combined effect of emergency environments and individual differences in terms of physiology and psychology.

TABLE I
Setting of Partial Parameters in BHSFM

Symbol	Description	Value
m_i	Pedestrian mass	$80\ kg$
v_i^0	Initial unit speed	$1\ ms^{-1}$
τ_i	Relaxation time	$0.5\ s$
A_i	Constant 1	$2\cdot 10^3\ N$
B_i	Constant 2	$0.08\ m$
r_i	Pedestrian radius	$0.25 \sim 0.35\ m$
k	Body elasticity coefficient	$1.2\cdot 10^5\ kgs^{-2}$
κ	Sliding friction coefficient	$2.4\cdot 10^5\ kgm^{-1}s^{-1}$
Δt	Time step	$0.04\ s$
Δ_P	Maximum fluctuation range	0.1
Δ_M	Maximum mutation	0.5
k_M	Mutation slope	0.1
γ_0	Non-emergency cooperation probability	0.95

B. Behavioral Heterogeneity-Based Social Force Model

In accordance with the behavioral heterogeneity coefficient defined above, the BHSFM is given by the following Langevin equation:

$$m_i \frac{d\mathbf{v}_i(t)}{dt} = \mathbf{f}_{id}^H + \sum_{j(\neq i)} \mathbf{f}_{ij} + \sum_W \mathbf{f}_{iW} \tag{15}$$

Here, the dynamic changes in pedestrian acceleration are dominated by the combined effect of forces.

The first term $\mathbf{f}_{id}^H$ reflects the self-driven force of pedestrians moving towards the destination:

$$\mathbf{f}_{id}^H = m_i \frac{H_i(t)\,v_i^0\mathbf{e}_i^0 - \mathbf{v}_i(t)}{\tau_i} \tag{16}$$

where pedestrian i adapts the actual speed $\mathbf{v}_i(t)$ to the desired speed $H_i(t)\,v_i^0$ and desired direction $\mathbf{e}_i^0$ within a certain relaxation τ_i, the coefficient $H_i(t)$ is added to reflect the behavioral heterogeneity by affecting the desired speed.

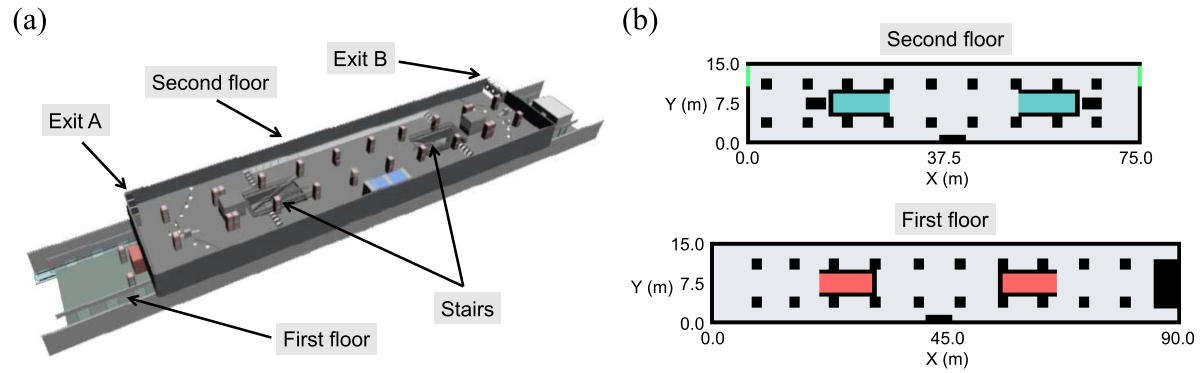

Fig. 1. Schematic diagram of the simulation scenario. (a) 3D Max structure diagram of Heping Xiqiao subway station in Beijing. (b) Simplified 2D floor plan of (a) for evacuation simulation. The first floor is 90 m length and 15 m width, and the second floor is 75 m length and 15 m width.

The second term $\mathbf{f}_{ij}$ illustrates the interaction force between pedestrian i and j:

$$\mathbf{f}_{ij} = A_i \exp\left[\left(r_{ij} - d_{ij}\right)/B_i\right]\mathbf{n}_{ij} + kg\left(r_{ij} - d_{ij}\right)\mathbf{n}_{ij} + \kappa g\left(r_{ij} - d_{ij}\right)\Delta v_{ji}^{t}\mathbf{t}_{ij} \quad (17)$$

where $A_i \exp\left[\left(r_{ij} - d_{ij}\right)/B_i\right]\mathbf{n}_{ij}$, $kg\left(r_{ij} - d_{ij}\right)\mathbf{n}_{ij}$, and $\kappa g\left(r_{ij} - d_{ij}\right)\Delta v_{ji}^{t}\mathbf{t}_{ij}$ correspond to a repulsive interaction force, a body force, and a sliding friction force between pedestrian i and j. In repulsive interaction force, A_i and B_i are constants, r_{ij} and d_{ij} respectively refer to the radius sum and the distance between the centroids of pedestrian i and j, and $\mathbf{n}_{ij}$ is the normalized vector pointing from pedestrian j to i. In body force and sliding friction force, $g(x)$ is zero if the two pedestrians do not touch each other, and otherwise it equals to x. k and κ are body elasticity coefficient and sliding friction coefficient, $\mathbf{t}_{ij}$ is the tangential direction, and $\Delta v_{ji}^{t} = \left(\mathbf{v}_j - \mathbf{v}_i\right)\cdot\mathbf{t}_{ij}$ is the tangential velocity difference.

The last term $\mathbf{f}_{iW}$ is generated by the interaction between pedestrian i and the walls:

$$\mathbf{f}_{iW} = A_i \exp\left[\left(r_i - d_{iW}\right)/B_i\right]\mathbf{n}_{iW} + kg\left(r_i - d_{iW}\right)\mathbf{n}_{iW} - \kappa g\left(r_i - d_{iW}\right)\left(\mathbf{v}_i\cdot\mathbf{t}_{iW}\right)\mathbf{t}_{iW} \quad (18)$$

where $A_i \exp\left[\left(r_i - d_{iW}\right)/B_i\right]\mathbf{n}_{iW}$, $kg\left(r_i - d_{iW}\right)\mathbf{n}_{iW}$, and $\kappa g\left(r_i - d_{iW}\right)\left(\mathbf{v}_i\cdot\mathbf{t}_{iW}\right)\mathbf{t}_{iW}$ represents a repulsive interaction force, a body force, and a sliding friction force between pedestrian i and the wall W. Here, d_{iW} is the distance to the wall W, $\mathbf{n}_{iW}$ and $\mathbf{t}_{iW}$ are the directions perpendicular and tangential to it, respectively.

IV. Numerical Experiments

A. Experiment Setup

Beijing, as the capital of China, adopts the Urban Rail Transit (URT) to transport an average of 10 million passengers per day [36]. As important transportation hubs, subway stations play a vital role in serving passengers on and off subways. However, a host of pedestrians gather in subway stations during specific periods (i.e., morning and evening peak periods) [37]. The increase in crowd density makes subway stations become potential high-risk areas of crowd disasters [38], especially when an emergency occurs [39], [40]. Thus, we select the Heping Xiqiao subway station in Beijing as a specific scenario to simulate the evacuation process using our model. Note that the emergency is assumed to occur after a train left the subway station, the existing passengers are taken as the simulation objects and new arrivals are prohibited.

The 3D Max structure diagram of Heping Xiqiao subway station is shown in Fig. 1(a), and we transform it into the 2D floor plan of two floors in Fig. 1(b). As the complexity of the real scenario, the influence of AFC gates, stairs and escalators is neglected and the pedestrian movement in these places is regarded as the same as that on platforms. The black bars or blocks represent walls or obstacles, and the green strip areas correspond to the two exits on the second floor. The first floor and second floor are connected by two stairs, in which red and cyan areas represent stairs up and down, respectively. In our case, the pedestrian spawning area is the remaining area in the 2D floor plan. Note that the 2D floor plan in Fig. 1(b) is scaled in proportion to the real scenario in Fig. 1(a), where each pixel corresponds to a square with a 0.15 m side.

Regarding the parameter setting in our simulation experiments, Table I indicates the values of partial parameters in the BHSFM, which are based on the existing literature. The scale factor θ_i in behavioral heterogeneity coefficient denotes the ratio of the desired speed in normal and the maximum desired speed in panic. Since the observed free speed under normal is $v_i^{nor} \approx 1\,m/s$ and under nervous or panic is $v_i^{\max} \geq 1.5\,m/s$ [41], thus a preliminary range of the scale factor can be obtained by $\theta_i \leq 0.67$. For simplicity, we hold $\theta_i = 0.5$ for each individual here. The remaining parameters in our model are given according to the simulation requirements in the following subsections.

B. Effect of Behavioral Heterogeneity Coefficient on Crowd Evacuation

To explore how the behavioral heterogeneity coefficient affects crowd evacuation, we adopt the BHSFM to simulate the collective motion of pedestrians in the subway station. In our case, the risk index is defined as $\lambda = 0.5$ to construct a moderate level of emergency. Given that crowds in the subway station are mixed by different types of pedestrians, we assume the physique coefficients of overall pedestrians follow the "approximate Gaussian distribution" at the initial time, where $\alpha = \beta = 4$, the location parameter $\mu = 0$ and the

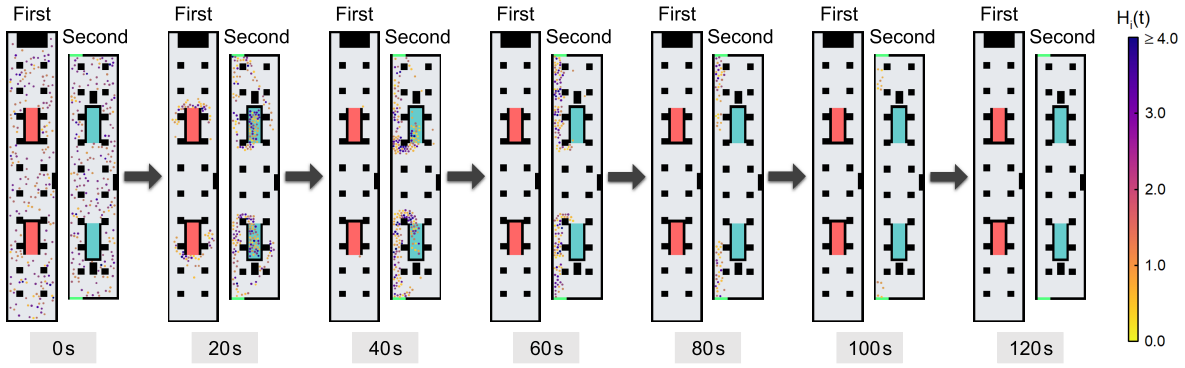

Fig. 2. Snapshots of crowd evacuation in the subway station under the effect of behavioral heterogeneity coefficient. The escaping pedestrians are represented by solid circles, the color of which reflects the value of behavioral heterogeneity coefficient.

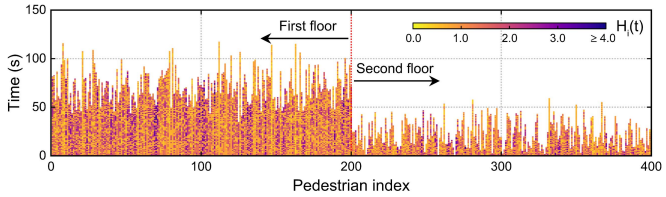

Fig. 3. Temporal evolution of behavioral heterogeneity coefficient for each pedestrian. The pedestrian index 0-200 and 200-400 respectively correspond to each pedestrian spawned on the first floor and the second floor at the initial time.

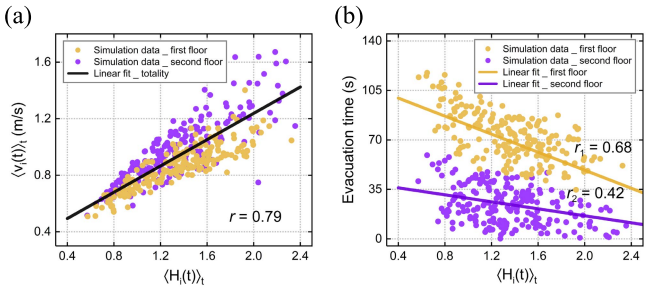

Fig. 4. Quantitative analysis of the effect of behavioral heterogeneity coefficient on crowd evacuation. (a) Relationship between the temporal average of behavioral heterogeneity coefficient and the temporal average of actual speed. (b) Relationship between the temporal average of behavioral heterogeneity coefficient and the evacuation time. The points with yellow and purple colors represent the simulation data corresponding to pedestrians spawned on the first floor and the second floor at the initial time, respectively.

scale parameter $\sigma = 3$. The attenuation rate of cooperation probability is set to $w_i = 1.25$, implying the probability of cooperation and competition is approximately equal when $\lambda = 0.5$. Besides, the initial number of pedestrians in the subway station is fixed as $N = 400$, in which each floor is randomly distributed with 200 pedestrians.

Based on the above settings, the snapshots of crowd evacuation in the subway station under the effect of behavioral heterogeneity coefficient are shown in Fig. 2. The solid circles with different colors correspond to the pedestrians with various values of behavioral heterogeneity coefficient. The impact of behavioral heterogeneity creates the difference in desired speed of each pedestrian, which forms a more realistic and elaborate evacuation process. Fig. 3 illustrates the temporal evolution of behavioral heterogeneity coefficient for each pedestrian. These dynamic characteristics are attributed to the combined effect of physiology and psychology attributes when surrounding environments and individuals change incessantly, in agreement with the viewpoints in the previous research [26].

To quantitatively analyze the effect of behavioral heterogeneity coefficient on crowd evacuation, the temporal average of behavioral heterogeneity coefficient for pedestrian i is calculated as follows:

$$\langle H_i(t)\rangle_t = \frac{1}{t_i - t_0}\sum_{t=t_0}^{t_i} H_i(t) \tag{19}$$

where t_i represents the exited time of pedestrian i. Analogously, the temporal average of actual speed for pedestrian i is given by the following:

$$\langle v_i(t)\rangle_t = \frac{1}{t_i - t_0}\sum_{t=t_0}^{t_i} v_i(t) \tag{20}$$

where $v_i(t) = \|\mathbf{v}_i(t)\|$ is the magnitude of actual speed. Notably, $\langle v_i(t)\rangle_t$ is found to have a high correlation $r = 0.79$ with $\langle H_i(t)\rangle_t$ in Fig. 4(a), which preliminarily demonstrates the interdependency between the actual escape speed and the behavioral heterogeneity coefficient. Fig. 4(b) illustrates this interdependency creates a relatively high correlation $r_1 = 0.68$ between the evacuation time of pedestrians spawned on the first floor with $\langle H_i(t)\rangle_t$, whereas pedestrians spawned on the second floor are limited by the overclose distance to exits, with a relatively weak correlation $r_2 = 0.42$. Nonetheless, these correlations still reveal a significant influence of behavioral heterogeneity coefficient on evacuation time.

Moreover, two evaluation indicators are defined to measure the differences in crowd evacuation simulated by SFM and BHSFM. Note that the desired speed for each pedestrian is equal to $v_i^0 = 2\,m/s$ in SFM. One is the temporal variance of actual speed for pedestrian i, which is expressed by:

$$Var_i[v_i(t)] = \frac{1}{t_i - t_0}\sum_{t=t_0}^{t_i}\left[v_i(t) - \langle v_i(t)\rangle_t\right]^2 \tag{21}$$

Another is the spatial variance of actual speed for overall pedestrians at time t, which reads:

$$Var_t[v_i(t)] = \frac{1}{N_t}\sum_{i=1}^{N_t}\left[v_i(t) - \langle v_i(t)\rangle_i\right]^2 \tag{22}$$

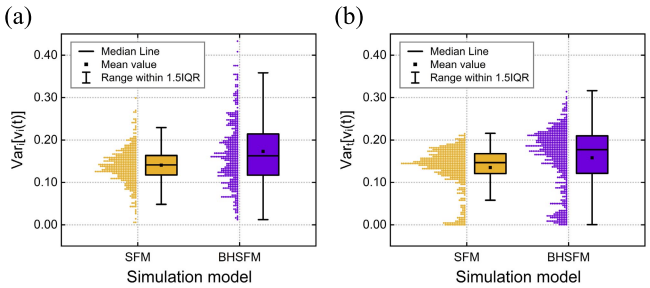

Fig. 5. Typical temporal-spatial differences of actual speed simulated by SFM and BHSFM. (a) Box plot of the temporal variance of actual speed. (b) Box plot of the spatial variance of actual speed. The points with yellow and purple colors constitute the distributions of simulation data corresponding to SFM and BHSFM, respectively.

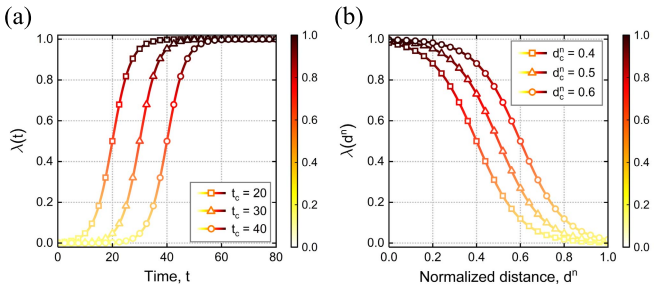

Fig. 6. Temporal-variant and spatial-variant risk indexes. (a) Risk index as a function of time without hazard source in the subway station. (b) Risk index as a function of the normalized distance to hazard source in the scenario. The gradient color scale marks the risky degree of dynamic risk indexes.

Here, N_t is the number of remaining pedestrians at time t, and $\langle\cdot\rangle_i$ denotes the average over remaining pedestrians. Both from the time and space dimensions in Fig. 5(a) and 5(b), larger variations of actual speed are shown by the box plots and the distributions of simulation data corresponding to BHSFM. Accordingly, the BHSFM performs more diversified actual speed differences compared with the SFM, which is caused by the integration of behavioral heterogeneity coefficient.

C. Influence of Dynamic Risk Indexes on Crowd Evacuation

Given that the risk index λ is considered as a constant in the previous experiment, whereas it tends to change dynamically in real life, and the temporal and spatial characteristics of risk perception exist throughout the evacuation process [42]. On the one hand, if the hazard source exists but is not in the subway station, it could conceivably be hypothesized that the risk index increases gradually with time t and then maintains invariant. This is similar to the situation that pedestrians progressively perceived the increasing degree of emergency, which is expressed in the form of a Sigmoid function:

$$\lambda(t) = \frac{\lambda_t^{\max}}{1 + \exp\left[-k_t\left(t - t_c\right)\right]} \tag{23}$$

where k_t is the ascending gradient, $\lambda_t^{\max}$ denotes the maximum risk index over time, and t_c is the moment corresponding to the slope increases the fastest. On the other hand, if a hazard source emerges in the subway station, there may exist a certain relevance between the risk index and the distance to it. A closer distance to the hazard source generally corresponds to a higher risk index. Thus, similar to Equation (23), a spatial expression that describes the risk index as a function of the normalized distance to hazard source is given by:

$$\lambda\left(d^n\right) = \frac{\lambda_d^{\max}}{1 + \exp\left[k_d\left(d^n - d_c^n\right)\right]} \tag{24}$$

Here, k_d is the descending gradient, $\lambda_d^{\max}$ holds the maximum risk index in the scenario, d^n indicates the normalized distance to the hazard source on this floor, and d_c^n is the normalized distance corresponding to the slope decreases the fastest.

To perform the curves of dynamic risk indexes, the values of relevant parameters are given below. We assume that the maximum risk index $\lambda_t^{\max} = 1$ over time, and the maximum risk index $\lambda_d^{\max} = 1$ when the pedestrian is closest to the hazard source. With the ascending gradient $k_t = 0.3$ and the descending gradient $k_d = 10$ we can reproduce the relatively reasonable dynamic tendency of these curves. The parameter t_c mainly determines the function phase of the temporal-variant risk index, we set its value as $t_c = 20, 30, 40$ and the curves of the temporal-variant risk index are depicted in Fig. 6(a). Another parameter d_c^n mainly affects the function concavity of the spatial-variant risk index, and Fig. 6(b) shows the curves of the spatial-variant risk index when the value is taken as $d_c^n = 0.4, 0.5, 0.6$. Note that the functions of dynamic risk indexes, $\lambda(t)$ and $\lambda\left(d_c^n\right)$, whose shapes can be adjusted by these parameters according to actual conditions.

To display the evacuation process affected by dynamic risk indexes, we select two cases in Fig. 6 that the temporal-variant risk index ($t_c = 30$) and the spatial-variant risk index ($d_c^n = 0.5$), other conditions remain the same as that in the previous section. Fig. 7(a) shows the escape behavior for each pedestrian is universally gentle in the initial phase due to the inconspicuous degree of emergency, while pedestrians impulsively accelerate to escape from the subway station during the risk index transiting from mild to severe level over time. This is consistent with empirical observations such as different escaping behaviors between the precursory period of an incident and the period after the alarm sounds. For another situation, the hazard source is located on the second floor, as shown by a red circular area in Fig. 7(b). Note that the spatial-variant risk index is assumed to target pedestrians on the second floor, while others on the first floor only perceive a mild risk level ($\lambda = 0.2$) since the hazard source is invisible to them. As we expect, pedestrians on the first floor hold relatively calm escape behavior, whereas pedestrians on the second floor have faster speed if they are closer to the hazard source. This triggers an interesting phenomenon that the pedestrians close to the hazard source push their front pedestrians for the purpose of quickly escaping the danger zone, similar to the crowd evacuation phenomenon when the World Trade Building collapsed in the 9/11 terror attacks.

Turning now to the experimental evidence on the temporal evolution of behavioral heterogeneity coefficient under different types of dynamic risk indexes. The increasing temporal-variant risk index exacerbates the fluctuation degree in physiology attributes and raises the stress level and the

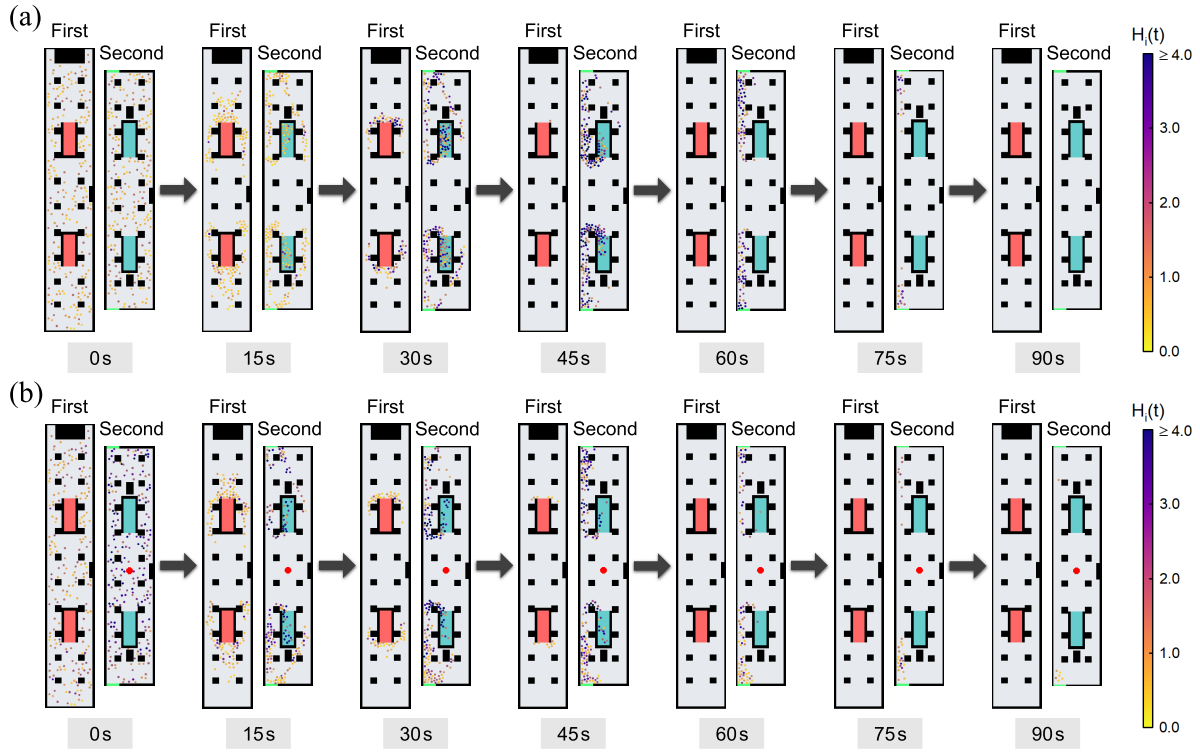

Fig. 7. Snapshots of crowd evacuation in the subway station under different types of dynamic risk indexes. (a) Under conditions of the temporal-variant risk index. (b) Under conditions of the spatial-variant risk index. The red circular area denotes the location of the hazard source. The escaping pedestrians are represented by solid circles, the color of which reflects the value of behavioral heterogeneity coefficient.

competition probability in psychology attributes. These factors collectively lead to a sudden enhancement of the behavioral heterogeneity coefficient during the phase from 20 s to 40 s in Fig. 8(a). Similarly, Fig. 8(b) displays the temporal evolution of behavioral heterogeneity coefficient under conditions of the spatial-variant risk index. The physiology and psychology attributes may further be stimulated to a more sensitive stage as pedestrians approach closer to the hazard source to some extent. The behavioral heterogeneity coefficients increase rapidly during this stage, while the period arriving at the stage is different for each pedestrian. This also accounts for the phenomenon emerging in Fig. 7(b), because the pedestrians near the hazard source are still at a stage with relatively higher behavioral heterogeneity coefficients.

Furthermore, the curves of evacuation efficiency in Fig. 9 reveal how different types of dynamic risk indexes affect the evacuation process. Under conditions of the temporal-variant risk index, the evacuation efficiency in Fig. 9(a) is relatively slow in the initial phase because pedestrians barely feel the urgency and keep the evacuation pattern in normal, whereas it grows rapidly in the subsequent phase since pedestrians perceive the intensely increasing risk, tallying with the circumstances in Fig. 7(a). Notably, the parameter t_c mainly affects the period, rather than the degree, of significant change in evacuation efficiency. Under conditions of the spatial-variant risk index, as shown in Fig. 9(b), the evacuation efficiency maintains a relatively smooth change tendency over time. The explanation for this might be that the existence of the hazard source promotes the evacuation efficiency on the second floor and avoids further congestion caused by the increase

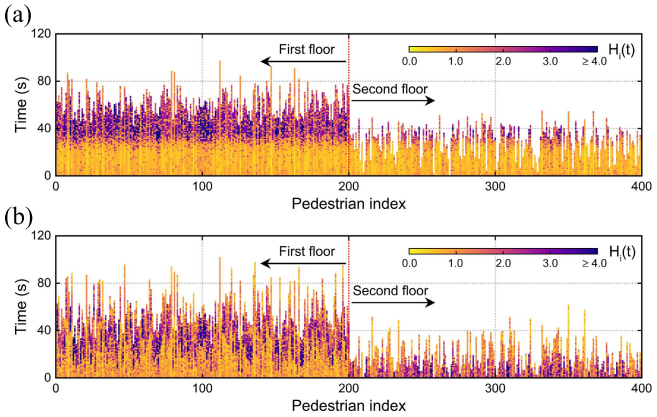

Fig. 8. Temporal evolution of behavioral heterogeneity coefficient for each pedestrian under different types of dynamic risk indexes. (a) Under conditions of the temporal-variant risk index. (b) Under conditions of the spatial-variant risk index. The pedestrian index 0-200 and 200-400 respectively correspond to each pedestrian on the first floor and the second floor at the initial time.

in the number of pedestrians. Besides, the parameter d_c^n has a primary influence on the degree of significant change in evacuation efficiency, with a larger d_c^n promotes the evacuation efficiency more evidently. In summary, the evacuation efficiency is dependent on the types and features of dynamic risk indexes to a great extent.

D. Analysis of Crowd Evacuation Under Different Numbers of Pedestrians

To our knowledge, the number of pedestrians at Heping Xiqiao subway station is different during various periods of

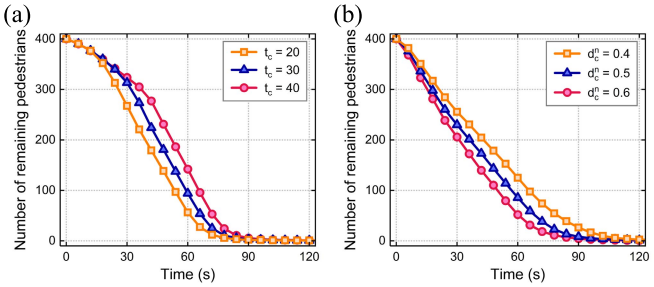

Fig. 9. Evacuation efficiency as a function of time under different types of dynamic risk indexes. (a) Under conditions of the temporal-variant risk index. (b) Under conditions of the spatial-variant risk index. The shape points represent the mean in 50 trials.

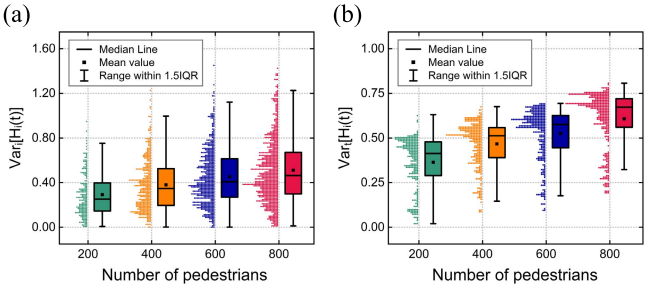

Fig. 10. Typical temporal-spatial differences of behavioral heterogeneity coefficient under different numbers of pedestrians. (a) Box plot of the temporal variance of behavioral heterogeneity coefficient. (b) Box plot of the spatial variance of behavioral heterogeneity coefficient. The points with various colors constitute the distributions of simulation data under different numbers of pedestrians.

the day. It is necessary to analyze the evacuation process under different numbers of pedestrians using the BHSFM, especially for the morning and evening peak periods in which the number increases sharply. Before conducting the numerical experiment, we first argue the setting of parameters in our simulation. The initial number of pedestrians in the subway station is set to $N = 200, 400, 600, 800$, where the number on each floor accounts for half of the total. Note that other parameters remain unchanged, including the risk index is fixed as $\lambda = 0.5$ for controlling the single variable.

The first issue in this numerical experiment seeks to determine how different numbers of pedestrians affect the variation degree of behavioral heterogeneity coefficient. For the evacuation process of a single pedestrian i, the temporal variance of behavioral heterogeneity coefficient can be quantified as a measurement indicator, which is given by the following:

$$Var_i\left[H_i\left(t\right)\right] = \frac{1}{t_i - t_0}\sum_{t=t_0}^{t_i}\left[H_i\left(t\right) - \left\langle H_i\left(t\right)\right\rangle_t\right]^2 \tag{25}$$

In this case, as shown in Fig. 10(a), the trend of the box plot reflects the increasing number of pedestrians corresponds to the overall growth of temporal variance, indicating that the behavioral heterogeneity coefficients transform more frequently. Additionally, regarding the evacuation process at a specific time t, the spatial variance of behavioral heterogeneity coefficient is defined as another quantitative indicator as follows:

$$Var_t\left[H_i\left(t\right)\right] = \frac{1}{N_t}\sum_{i=1}^{N_t}\left[H_i\left(t\right) - \left\langle H_i\left(t\right)\right\rangle_i\right]^2 \tag{26}$$

From a spatial aspect in Fig. 10(b), the increasing trend of spatial variance reveals a larger difference in behavioral heterogeneity coefficients as the number of pedestrians raises, in agreement with the realistic situation.

The next target of this experiment is concerned with the distribution of displacements, where the displacement is regarded as the distance between two subsequent stops (defined by the actual speed below $0.1\,m/s$). Fig. 11 shows there exists a power law of displacements in the double logarithmic coordinate system, consistent with the previous findings [16]. Owing to the fact the increasing number of pedestrians creates a greater degree of congestion, the exponent increment of power law reveals that more small-scale displacements are generated, which is reflected in the simulation process of SFM and BHSFM. However, the BHSFM produces higher frequencies of small-scale displacements compared with the SFM, the potential explanation for it might be related to more pushing behaviors caused by the expanded temporal-spatial differences in behavioral heterogeneity coefficients, which also echoes with the observed traffic perturbations affected by the speed variability [43].

The direct impact of higher frequencies of small-scale displacements is to trigger more severe extrusions and even lead to crowd disasters. Therefore, finding the periods and areas of a potential crowd disaster is significant for the management of crowd evacuation in specific scenarios [44]. Here, several critical definitions are introduced for our analysis. The local density at place $\mathbf{x}$ and time t is expressed by:

$$\rho\left(\mathbf{x}, t\right) = \sum_i f\left(d_{i\mathbf{x}}, t\right) \tag{27}$$

where $d_{i\mathbf{x}}$ is the distance between place $\mathbf{x}$ and pedestrian i, and $f\left(d\right)$ is a Gaussian distance-dependent weight function:

$$f\left(d\right) = \frac{1}{\pi R^2}\exp\left(-\frac{d^2}{R^2}\right) \tag{28}$$

where R denotes a measurement parameter, the reasonable value of which is $R = 0.7\,m$. Besides, the local speed is defined via the weighted average as follows:

$$V\left(\mathbf{x}, t\right) = \frac{\sum_i \left\|\mathbf{v}_i\right\| f\left(d_{i\mathbf{x}}, t\right)}{\sum_i f\left(d_{i\mathbf{x}}, t\right)} \tag{29}$$

Regarding extra details of the above definitions see [16], [17].

To determine the periods of a potential crowd disaster during the evacuation process, the "pressure" [16] as a function of time t is calculated by:

$$P\left(t\right) = \rho\left(t\right) Var_t\left[V\left(\mathbf{x}, t\right)\right] \tag{30}$$

Here, $\rho\left(t\right) = \left\langle\rho\left(\mathbf{x}, t\right)\right\rangle_{\mathbf{x}}$ is the spatial average of the local density, and $Var_t\left[V\left(\mathbf{x}, t\right)\right] = \left\langle\left[V\left(\mathbf{x}, t\right) - \left\langle V\left(\mathbf{x}, t\right)\right\rangle_{\mathbf{x}}\right]^2\right\rangle_{\mathbf{x}}$ is the spatial variance of the local speed at time t. Fig. 12 presents the duration of high "pressure" values exists on the second floor is much longer than that on the first floor,

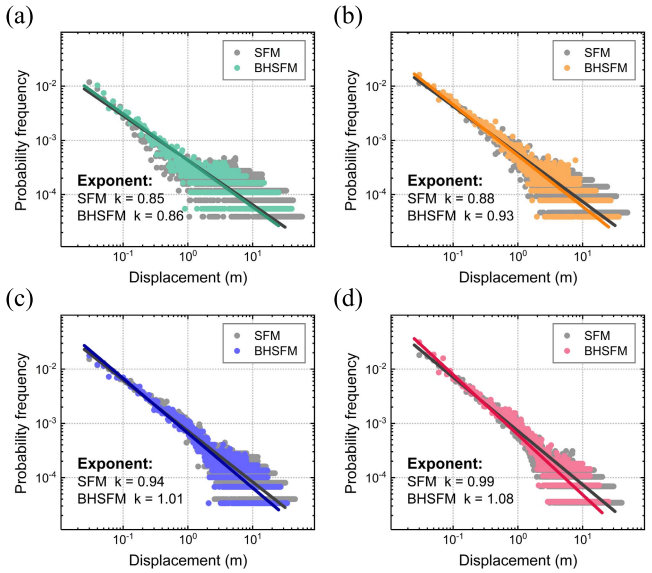

Fig. 11. Distribution of displacements (i.e., location changes between two subsequent stops, defined by $\|\mathbf{v}_i\| < 0.1\ m/s$) simulated by SFM and BHSFM under different numbers of pedestrians. (a) $N = 200$. (b) $N = 400$. (c) $N = 600$. (d) $N = 800$. The double logarithmic representation reveals the power law for different numbers of pedestrians.

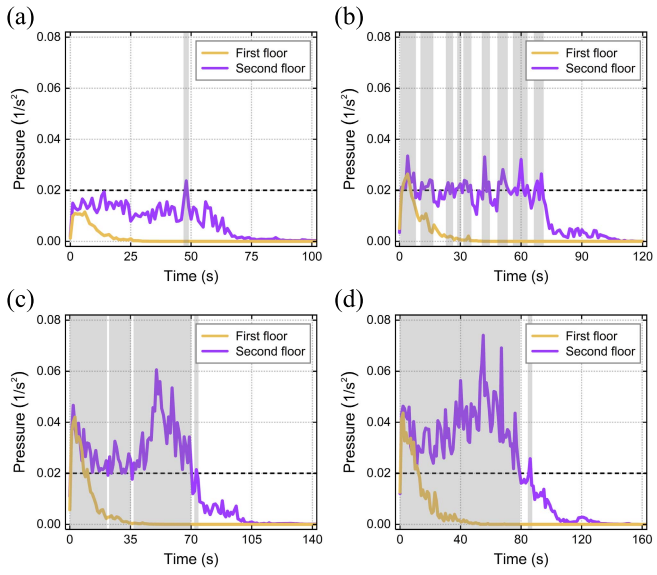

Fig. 12. Temporal dynamics of "pressure" under different numbers of pedestrians. (a) $N = 200$. (b) $N = 400$. (c) $N = 600$. (d) $N = 800$. The black dashed line corresponds to a critical value, in which the "crowd turbulent" phenomenon was observed when the "pressure" exceeds the value $0.02/s^2$. The shaded areas mark the periods when the critical value are exceeded.

because more serious congestion is caused by the influx of pedestrians from the first floor. Note that an implication of the black dashed line is the critical value, and the potential "crowd turbulent" phenomenon might be observed when the "pressure" exceeds it [16], the periods of which are marked by the shaded areas. With successive increase in the number of pedestrians, these periods appear more frequently and almost emerge throughout the first half of the evacuation process when $N \geq 600$ in Fig. 12(c) and 12(d). These results have important guidances for determining the periods of a potential crowd disaster under different numbers of pedestrians.

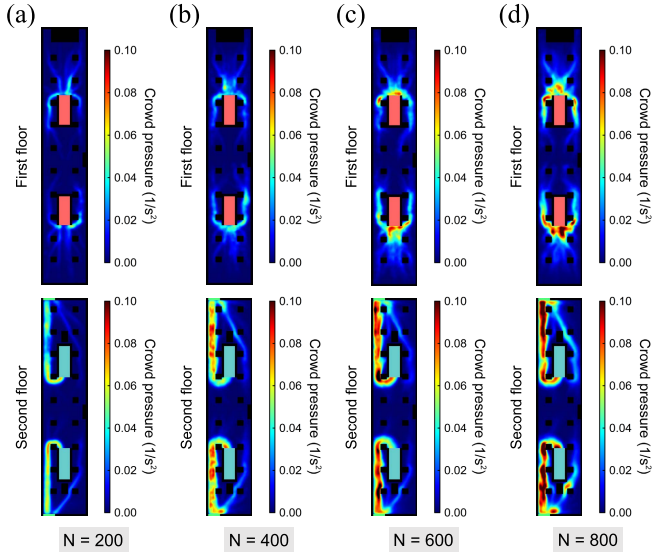

Fig. 13. Spatial characterization of "crowd pressure" under different numbers of pedestrians. (a) $N = 200$. (b) $N = 400$. (c) $N = 600$. (d) $N = 800$. The color coding indicates the "crowd pressure" values. Note that the exit and stair areas are not considered, whose color coding denotes the original color.

Turning to the space dimension, the "crowd pressure" [17] that used to ascertain the areas of a potential crowd disaster is given by the following:

$$C(\mathbf{x}) = \rho(\mathbf{x})\, Var_{\mathbf{x}}[V(\mathbf{x}, t)] \tag{31}$$

where $\rho(\mathbf{x}) = \langle \rho(\mathbf{x}, t) \rangle_t$ is the temporal average of the local density, and $Var_{\mathbf{x}}[V(\mathbf{x}, t)] = \left\langle \left[V(\mathbf{x}, t) - \langle V(\mathbf{x}, t) \rangle_t \right]^2 \right\rangle_t$ is the temporal variance of the local speed at place $\mathbf{x}$. Fig. 13 shows the spatial characterization of "crowd pressure" under different numbers of pedestrians. It is obvious that the areas of relatively higher "crowd pressure" are concentrated near the entrance of the staircase on the first floor and the unilateral corridor from the export of the staircase to the exit on the second floor. Notably, the areas with a high risk of falling (in dark red) are expanded as the number of pedestrians increases, denoting the areas of a potential crowd disaster. The identification of these high-risk areas provides relevant evidence for formulating reasonable evacuation schemes in this subway station.

V. Conclusion

In this paper, the BHSFM is designed to provide a general framework for describing the pedestrian heterogeneity during evacuation process. Specifically, a behavioral heterogeneity coefficient, involving emergency environments and individual differences, is incorporated into the SFM to reveal the heterogeneity characteristics of pedestrian behavior. After conducting numerical experiments in the simulation scenario of Heping Xiqiao subway station, the most primary conclusions emerging from this study are summarized as follows:

(1) The linear interdependency between the actual escape speed and the behavioral heterogeneity coefficient has a significant influence on the evacuation time of pedestrians, which achieves a more reasonable and elaborate evacuation process in

the subway station by introducing the behavioral heterogeneity as a quantitative indicator.

(2) There emerge some interesting evacuation phenomena by integrating temporal-spatial dynamic risk indexes, such as the impulsive acceleration behavior during the risk index transiting from mild to severe level over time, and the pushing behavior from pedestrians close to the hazard source to the pedestrians ahead of them.

(3) Compared with the SFM, our model produces higher frequencies of small-scale displacements due to more pushing behaviors, and it becomes more prominent as the number of pedestrians increases. Besides, the BHSFM indicates the periods and areas of a potential crowd disaster for the crowd management during evacuation process.

The above conclusions contribute in several ways to our understanding of pedestrian heterogeneity and provide a basis for guiding crowd evacuation in specific scenarios. In terms of route planning, designing fast and dedicated evacuation routes for those pedestrians with lower behavioral heterogeneity coefficients is worth deeply considering [45]. Regarding the evacuation schemes, assigning reasonable emergency signs is essential to reduce the periods and areas of a potential crowd disaster [46]. Apart from the management of crowd evacuation, our model also sheds new light on other practical applications, such as improving the building structures by considering the impact of collective behavior [47], simulating the human-vehicle interaction phenomenon under the pushing behavior of pedestrians at the rear, as well as inspiring the heterogeneous expressions of pedestrian groups [48], vehicles [49], and roads [50] for more suitable traffic control in complicated scenarios. These viewpoints have significant implications for the insights of distinctive collective patterns by abandoning the traditional homogeneity notions.

Although the BHSFM has been proved to be an effective model for simulating crowd evacuation, its limitations are listed as follows. First, this model ignores the behavioral heterogeneity in terms of information perception [51], [52], such as visual and auditory information, which can be regarded as a high-dimensional interaction process between the environment and individuals. Second, the dynamic risk index is assumed as a simplified Sigmoid function of time or space, whereas the dynamics of emergency environment may be quite complicated in real situations, therefore combining with the research (i.e., fire spread, gas diffusion) in other fields is necessary [53]. Notwithstanding these limitations, this work offers valuable insights into the refined expression of behavioral heterogeneity in modeling crowd motion. In the future, the precise mechanism of heterogeneity in human crowds remains to be elucidated. We also expect that our model can open new perspectives in establishing more realistic models of collective motion.

REFERENCES

[1] M. Zhou, H. Dong, B. Ning, and F. Wang, "Recent development in pedestrian and evacuation dynamics: Bibliographic analyses, collaboration patterns, and future directions," *IEEE Trans. Computat. Social Syst.*, vol. 5, no. 4, pp. 1034–1048, Dec. 2018.

[2] H. Dong, M. Zhou, Q. Wang, X. Yang, and F.-Y. Wang, "State-of-the-art pedestrian and evacuation dynamics," *IEEE Trans. Intell. Transp. Syst.*, vol. 21, no. 5, pp. 1849–1866, May 2020.

[3] D. M. J. Lazer *et al.*, "Computational social science: Obstacles and opportunities," *Science*, vol. 369, no. 6507, pp. 1060–1062, Aug. 2020.

[4] L. F. Henderson, "The statistics of crowd fluids," *Nature*, vol. 229, no. 5284, pp. 381–383, 1971.

[5] D. Helbing, "A fluid dynamic model for the movement of pedestrians," *Complex Syst.*, vol. 6, no. 5, pp. 391–415, 1992.

[6] N. Bain and D. Bartolo, "Dynamic response and hydrodynamics of polarized crowds," *Science*, vol. 363, no. 6422, pp. 46–49, Jan. 2019.

[7] N. Bellomo and C. Dogbe, "On the modelling crowd dynamics from scaling to hyperbolic macroscopic models," *Math. Models Methods Appl. Sci.*, vol. 18, pp. 1317–1345, Aug. 2008.

[8] J. MacGregor Smith, "State-dependent queueing models in emergency evacuation networks," *Transp. Res. B, Methodol.*, vol. 25, no. 6, pp. 373–389, Dec. 1991.

[9] D. Helbing and P. Molnar, "Social force model for pedestrian dynamics," *Phys. Rev. E, Stat. Phys. Plasmas Fluids Relat. Interdiscip. Top.*, vol. 51, no. 5, pp. 4282–4286, 1995.

[10] A. Kirchner and A. Schadschneider, "Simulation of evacuation processes using a bionics-inspired cellular automaton model for pedestrian dynamics," *Phys. A, Stat. Mech. Appl.*, vol. 312, nos. 1–2, pp. 260–276, 2002.

[11] M. Muramatsu, T. Irie, and T. Nagatani, "Jamming transition in pedestrian counter flow," *Phys. A, Stat. Mech. Appl.*, vol. 267, nos. 3–4, pp. 487–498, 1999.

[12] T. Vicsek and A. Zafeiris, "Collective motion," *Phys. Rep.*, vol. 517, no. 3, pp. 71–140, 2012.

[13] D. Helbing, L. Buzna, A. Johansson, and T. Werner, "Self-organized pedestrian crowd dynamics: Experiments, simulations, and design solutions," *Transp. Sci.*, vol. 39, no. 1, pp. 1–24, 2005.

[14] D. Helbing, I. Farkas, and T. Vicsek, "Simulating dynamical features of escape panic," *Nature*, vol. 407, pp. 487–490, Sep. 2000.

[15] D. Helbing, I. J. Farkas, and T. Vicsek, "Freezing by heating in a driven mesoscopic system," *Phys. Rev. Lett.*, vol. 84, no. 6, pp. 1240–1243, 2000.

[16] D. Helbing, A. Johansson, and H. Z. Al-Abideen, "Dynamics of crowd disasters: An empirical study," *Phys. Rev. E, Stat. Phys. Plasmas Fluids Relat. Interdiscip. Top.*, vol. 75, no. 4, Apr. 2007, Art. no. 046109.

[17] M. Moussaïd, D. Helbing, and G. Theraulaz, "How simple rules determine pedestrian behavior and crowd disasters," *Proc. Nat. Acad. Sci. USA*, vol. 108, no. 17, pp. 6884–6888, 2011.

[18] K. Szwaykowska, L. Mier-y-Teran Rome, and I. B. Schwartz, "Collective motions of heterogeneous swarms," *IEEE Trans. Autom. Sci. Eng.*, vol. 12, no. 3, pp. 810–818, Jul. 2015.

[19] M. Dorigo, G. Theraulaz, and V. Trianni, "Reflections on the future of swarm robotics," *Sci. Robot.*, vol. 5, no. 49, Dec. 2020, Art. no. eabe4385.

[20] S. Cao, J. Zhang, D. Salden, J. Ma, C. Shi, and R. Zhang, "Pedestrian dynamics in single-file movement of crowd with different age compositions," *Phys. Rev. E, Stat. Phys. Plasmas Fluids Relat. Interdiscip. Top.*, vol. 94, no. 1, Jul. 2016, Art. no. 012312.

[21] A. Fujita, C. Feliciani, D. Yanagisawa, and K. Nishinari, "Traffic flow in a crowd of pedestrians walking at different speeds," *Phys. Rev. E, Stat. Phys. Plasmas Fluids Relat. Interdiscip. Top.*, vol. 99, no. 6, Jun. 2019, Art. no. 062307.

[22] R. Subaih, M. Maree, M. Chraibi, S. Awad, and T. Zanoon, "Experimental investigation on the alleged gender-differences in pedestrian dynamics: A study reveals, no. gender differences in pedestrian movement behavior," *IEEE Access*, vol. 8, pp. 33748–33757, 2020.

[23] X. Guo, J. Chen, Y. Zheng, and J. Wei, "A heterogeneous lattice gas model for simulating pedestrian evacuation," *Phys. A, Stat. Mech. Appl.*, vol. 391, no. 3, pp. 582–592, Feb. 2012.

[24] P. Hrabák and M. Bukáček, "Influence of agents heterogeneity in cellular model of evacuation," *J. Comput. Sci.*, vol. 21, pp. 486–493, Jul. 2017.

[25] X. Zheng, T. Zhong, and M. Liu, "Modeling crowd evacuation of a building based on seven methodological approaches," *Building Environ.*, vol. 44, no. 3, pp. 437–445, 2009.

[26] R. F. Cao *et al.*, "Development of an evacuation model considering the impact of stress variation on evacuees under fire emergency," *Saf. Sci.*, vol. 138, Jun. 2021, Art. no. 105232.

[27] L. Ma, B. Chen, X. Wang, Z. Zhu, R. Wang, and X. Qiu, "The analysis on the desired speed in social force model using a data driven approach," *Phys. A, Stat. Mech. Appl.*, vol. 525, pp. 894–911, Jul. 2019.

[28] X. Chen, M. Treiber, V. Kanagaraj, and H. Li, "Social force models for pedestrian traffic—State of the art," *Transp. Rev.*, vol. 38, no. 5, pp. 625–653, Nov. 2017.

[29] W. Wu, M. Chen, J. Li, B. Liu, and X. Zheng, "An extended social force model via pedestrian heterogeneity affecting the self-driven force," *IEEE Trans. Intell. Transp. Syst.*, early access, May 5, 2021, doi: 10.1109/TITS.2021.3074914.
[30] N. Bellomo and L. Gibelli, "Toward a mathematical theory of behavioral-social dynamics for pedestrian crowds," *Math. Models Methods Appl. Sci.*, vol. 25, no. 13, pp. 2417–2437, 2015.
[31] A. Shipman and A. Majumdar, "Fear in humans: A glimpse into the crowd-modeling perspective," *Transp. Res. Rec., J. Transp. Res. Board*, vol. 2672, no. 1, pp. 183–197, Aug. 2018.
[32] M. H. Zaki and T. Sayed, "Using automated walking gait analysis for the identification of pedestrian attributes," *Transp. Res. C, Emerg. Technol.*, vol. 48, pp. 16–36, Nov. 2014.
[33] J. M. Hausdorff, "Gait dynamics, fractals and falls: Finding meaning in the stride-to-stride fluctuations of human walking," *Hum. Movement Sci.*, vol. 26, no. 4, pp. 555–589, 2007.
[34] C. A. Hill, S. Suzuki, R. Polania, M. Moisa, J. P. O'Doherty, and C. C. Ruff, "A causal account of the brain network computations underlying strategic social behavior," *Nature Neurosci.*, vol. 20, no. 8, pp. 1142–1149, Jul. 2017.
[35] C. L. Bethel and R. R. Murphy, "Survey of non-facial/non-verbal affective expressions for appearance-constrained robots," *IEEE Trans. Syst., Man, Cybern., C, Appl. Rev.*, vol. 38, no. 1, pp. 83–92, Jan. 2008.
[36] J. Feng, X. Li, B. Mao, Q. Xu, and Y. Bai, "Weighted complex network analysis of the Beijing subway system: Train and passenger flows," *Phys. A, Stat. Mech. Appl.*, vol. 474, pp. 213–223, May 2017.
[37] C. Chen, J. Chen, and J. Barry, "Diurnal pattern of transit ridership: A case study of the New York City subway system," *J. Transp. Geography*, vol. 17, no. 3, pp. 176–186, 2009.
[38] M. Zhou, H. Dong, Y. Zhao, P. A. Ioannou, and F. Y. Wang, "Optimization of crowd evacuation with leaders in urban rail transit stations," *IEEE Trans. Intell. Transport. Syst.*, vol. 20, no. 12, pp. 4476–4487, Dec. 2019.
[39] G. Jeon and W. Hong, "Characteristic features of the behavior and perception of evacuees from the Daegu subway fire and safety measures in an underground fire," *J. Asian Archit. Building Eng.*, vol. 8, no. 2, pp. 415–422, Nov. 2009.
[40] A. Shvetsov, S. Shvetsova, V. A. Kozyrev, V. A. Spharov, and N. M. Sheremet, "The 'car-bomb' as a terrorist tool at metro stations, railway terminals and airports," *J. Transp. Secur.*, vol. 10, nos. 1–2, pp. 31–43, Dec. 2016.
[41] D. Helbing, I. J. Farkas, P. Molnar, and T. Vicsek, "Simulation of pedestrian crowds in normal and evacuation situations," *Pedestrian Evacuation Dyn.*, vol. 21, no. 2, pp. 21–58, 2002.
[42] L. K. Siebeneck and T. J. Cova, "Spatial and temporal variation in evacuee risk perception throughout the evacuation and return-entry process," *Risk Anal.*, vol. 32, no. 9, pp. 1468–1480, Mar. 2012.
[43] M. Moussaïd *et al.*, "Traffic instabilities in self-organized pedestrian crowds," *PLoS Comput. Biol.*, vol. 8, no. 3, Mar. 2012, Art. no. e1002442.
[44] C. Feliciani and K. Nishinari, "Measurement of congestion and intrinsic risk in pedestrian crowds," *Transp. Res. C, Emerg. Technol.*, vol. 91, pp. 124–155, Jun. 2018.
[45] Z. Han, W. Weng, Q. Zhao, X. Ma, Q. Liu, and Q. Huang, "Investigation on an integrated evacuation route planning method based on real-time data acquisition for high-rise building fire," *IEEE Trans. Intell. Transp. Syst.*, vol. 14, no. 2, pp. 782–795, Jun. 2013.
[46] M. Zhou, H. Dong, X. Wang, X. Hu, and S. Ge, "Modeling and simulation of crowd evacuation with signs at subway platform: A case study of Beijing subway stations," *IEEE Trans. Intell. Transp. Syst.*, early access, Oct. 20, 2020, doi: 10.1109/TITS.2020.3027542.
[47] N. Pinter-Wollman, A. Penn, G. Theraulaz, and S. M. Fiore, "Interdisciplinary approaches for uncovering the impacts of architecture on collective behaviour," *Phil. Trans. Roy. Soc. B, Biol. Sci.*, vol. 373, no. 1753, Jul. 2018, Art. no. 20170232.
[48] W. Xie, E. W. M. Lee, T. Li, M. Shi, R. Cao, and Y. Zhang, "A study of group effects in pedestrian crowd evacuation: Experiments, modelling and simulation," *Saf. Sci.*, vol. 133, Jan. 2021, Art. no. 105029.
[49] D. Helbing and B. Tilch, "Generalized force model of traffic dynamics," *Phys. Rev. E, Stat. Phys. Plasmas Fluids Relat. Interdiscip. Top.*, vol. 58, no. 1, pp. 133–138, 1998.
[50] D. Helbing, J. Keltsch, and P. Molnár, "Modelling the evolution of human trail systems," *Nature*, vol. 388, no. 6637, pp. 47–50, Jul. 1997.
[51] H. E. A. MacGregor, J. E. Herbert-Read, and C. C. Ioannou, "Information can explain the dynamics of group order in animal collective behaviour," *Nature Commun.*, vol. 11, no. 1, pp. 1–8, Jun. 2020.
[52] R. Bastien and P. Romanczuk, "A model of collective behavior based purely on vision," *Sci. Adv.*, vol. 6, no. 6, Feb. 2020, Art. no. eaay0792.
[53] Z. Dou *et al.*, "Review on the emergency evacuation in chemicals-concentrated areas," *J. Loss Prevention Process Industries*, vol. 60, pp. 35–45, Jul. 2019.

Wenhan Wu received the B.S. degree from the School of Automation, Central South University, Changsha, China, in 2019. He is currently pursuing the Ph.D. degree in control science and engineering with Tsinghua University, Beijing, China. His current research interests include collective behavior, emergency evacuation, and pedestrian group dynamics.

Jinghai Li received the B.S. degree in automation and the M.S. degree in control science and engineering from Tianjin University, Tianjin, China, in 2009 and 2016, respectively. He is currently pursuing the Ph.D. degree in control science and engineering with Tsinghua University, Beijing, China. His current research interests include crowd dynamics, planning, and control of robotic systems, and adaptive systems.

Wenfeng Yi received the B.S. degree from the School of Astronautics, Beihang University, Beijing, China, in 2019. He is currently pursuing the Ph.D. degree in control science and engineering with Tsinghua University, Beijing. His current research interests include collective behavior, emergency evacuation, and pedestrian queueing dynamics.

Xiaoping Zheng received the B.S. degree from the Chengdu University of TCM, Chengdu, China, in 1995, and the Ph.D. degree from Sichuan University, Chengdu, in 2003.

From 2004 to 2006, he was a Post-Doctoral Researcher with the School of Management, Fudan University, Shanghai, China. From 2006 to 2013, he was a Professor with the Institute of Safety Management, Beijing University of Chemical Technology, Beijing, China. He is currently a Professor with the Department of Automation, Tsinghua University, Beijing. He was a 973 Chief Scientist in 2011. His current research interests include large-scale crowd evacuation, evolutionary game theory, and terahertz technology. He was a recipient of the National Science Fund for Distinguished Young Scholars in 2012.